UDC 621.365.51 https://doi.org/10.20998/2074-272X.2024.1.07

A.A. Shcherba, O.D. Podoltsev, N.I. Suprunovska, R.V. Bilianin, T.Yu. Antonets, I.M. Masluchenko

Modeling and analysis of electro-thermal processes in installations for induction heat treatment of aluminum cores of power cables

Introduction. *The development of the electric power industry is directly related to the improvement of cable lines. Cable lines meet modern requirements for reliability, they are increasingly used.* ***Problem***. *Currently, power cables with an aluminum multi-conductor core, which requires heat treatment - an annealing process at the stage of the technological manufacturing process, are widespread. This process makes it possible to desirably reduce the electrical resistance of the wire and increase its flexibility. For effective use of induction heating during annealing of an aluminum core, it is necessary to determine the optimal frequency of the power source of the inductor. Considering the long length of the inductor and the large number of its turns, the numerical calculation of the electromagnetic field, which is necessary for calculating the equivalent electrical parameters of the turns of the inductor and its efficiency, requires significant computer resources. The* ***goal*** *is to develop a computer model for calculating electro-thermal processes in an induction plant for heating (up to the annealing temperature) an aluminum core of a power cable moving in the magnetic field of a long multi-turn inductor, as well as obtaining frequency dependences of the equivalent R, L parameters of such an inductor and determining the optimal the value of the frequency of the power source, which corresponds to the maximum value of the electrical efficiency of the inductor.* ***Methodology***. *The mathematical model was developed to analyze the coupled electromagnetic and thermal processes occurring in a core moving in a time-harmonic magnetic field of an inductor at a constant speed. The differential equations for the electromagnetic and temperature fields, taking into account the boundary conditions, represent a coupled electro-thermal problem that was solved numerically by the finite element method using the Comsol software package. For a detailed analysis of the electromagnetic processes in the inductor, an additional problem was considered at the level of the elementary cell, which includes one turn of the inductor and a fragment of the core located near this turn.* ***Results***. *According to the results of the calculation of the electromagnetic field in the area of the elementary cell, the equivalent electrical parameters of one turn of the inductor and the entire multi-turn inductor were calculated depending on the frequency of the electric current. The frequency dependences of the electrical efficiency of the inductor were calculated.* ***Originality***. *Taking into account the design features of the inductor (its long length and large number of turns), the method of multiscale modeling was used. Electro-thermal processes in the core were studied at the macro level, and the distribution of the electromagnetic field and electric current density in the cross-section of the massive copper turn of the inductor was calculated at the micro level – at the level of an elementary cell containing only one turn of the inductor. The frequency dependences of the equivalent R, L parameters of the inductor, taking into account the skin effect, the proximity effect, and the geometric effect, were obtained, and the quantitative influence of the electric current frequency on these effects was studied.* ***Practical value***. *The dependence of the electrical efficiency of the inductor on the frequency of the power source was obtained and it was shown that for effective heating of an aluminum core with a diameter of 28 mm, the optimal value of the frequency is in the range of 1–2 kHz, and at the same time the electrical efficiency reaches values of* η_{ind} *= 0.3–0.33, respectively.* References 31, figures 10, table 1.

Key words: **electromagnetic processes, induction heat treatment, aluminum conductive core, power cables, multiscale modeling, current frequency, inductor efficiency**.

У роботі досліджено електромагнітні та теплові процеси в установках індукційного нагрівання алюмінієвої жили силових кабелів та умови реалізації технології її відпалювання. При математичному моделюванні вказаних процесів ураховано такі конструктивні особливості індуктора, як його значна довжина і відповідно велика кількість його витків, що викликало необхідність використати метод мультимасштабного моделювання. При цьому на макрорівні розраховувались електротеплові процеси в жилі, що рухалась у магнітному полі індуктора, а на мікрорівні (тобто на рівні елементарної комірки, що має лише один виток індуктора) визначався розподіл електромагнітного поля та густини електричного струму в перерізі масивного мідного витка індуктора з урахуванням особливостей його конструкції. На обох рівнях у роботі використовувався чисельний метод скінченних елементів, реалізований в пакеті програм Comsol. За результатами розрахунку електромагнітного поля на рівні елементарної комірки, отримано частотні залежності еквівалентних R, L параметрів індуктора із урахуванням скін-ефекту, ефекту близькості та геометричного ефекту. Досліджено кількісний вплив частоти електричного струму на ці ефекти та отримано залежність електричного ККД індуктора від частоти джерела електроживлення. Показано, що для ефективного нагрівання алюмінієвої жили діаметром 28 мм оптимальне значення частоти знаходиться в діапазоні 1–2 кГц, в якому електричний ККД може досягати значень η_{ind} *= 0,3–0,33.* Бібл. 31, рис. 10, табл. 1.

Ключові слова: **електромагнітні процеси, індукційна термообробка, алюмінієва струмопровідна жила, силові кабелі, мультимасштабне моделювання, частота струму, ККД індуктора.**

Introduction. For a long time, innovative research and development in the domestic electric power industry was aimed at the development of decentralized local Microgrid electrical systems [1–4], which use dynamic regulation of the power balance of distributed sources of electricity in conditions of non-stationary consumption by industrial and residential complexes and objects without taking into account electrophysical features of structural elements of cable and conductor products of overhead [5] and cable power transmission lines (PTLs) [6–8].

In the 21st century, the industrialized countries of the world began to use self-supporting insulated wires (SIWs) with a reinforced current-conducting core made of electrotechnical alloys of the «TA» brand (hard aluminum) and nanomodified («cross-linked») polyethylene (LPE) insulation in overhead power lines. In Ukraine, YUZHCABLE WORKS, PJSC, Kharkiv, Ukraine was the first to master the industrial production of SIWs [5]. Their implementation in single-phase and three-phase PTLs with voltage of up to 1 kV made it possible to twist phase and neutral wires into one bundle, which reduced the running inductance and voltage drop several times. The land acquisition area for the construction of PTLs has significantly decreased, and

their repair and maintenance has been simplified. In such PTLs, short circuits do not occur during bad weather and other external influences, which increased the safety and reliability of power supply systems of responsible energy consumers [5]. A significant reduction in the inductance of overhead PTLs with SIWs even led to the appearance of studies on the feasibility of using capacitive reactive power compensators in them [9].

YUZHCABLE WORKS, PJSC also mastered the serial production of innovative domestic power cables with three-layer LPE insulation and mainly aluminum core, which ensured the intensive development of the construction and use of underground cable PTLs in Ukraine with voltage of up to 330 kV and power of hundreds to thousands MVA, which are more reliable and protected from any external influences [7] than overhead PTLs even with SIWs [5]. Moreover, in the production of current-conducting cores of cables, alloys of the «TA» brand are also mostly used.

However, the problem of speeding up work on restoration of power supply of critical infrastructure objects using undamaged cable channels and trays is currently intensifying in Ukraine, for the solution of which it is desirable to use cables with a core of increased plasticity and current conductivity.

Modern power cables with LPE insulation and multi-wire copper core have the highest plasticity and specific electrical conductivity [10–12]. Such cables are used in power systems of many countries of the world. But the lack of own copper deposits in Ukraine and the high price of its import limit the possibility of its wide use in the domestic electric power industry.

In our country, power cables with a copper current-conducting core are mainly used in pulse electrical engineering, in particular in the discharge circuits of linear [13] and nonlinear [14] capacitive electricity storage devices of electric discharge units for the implementation of pulse spark plasma processes of obtaining micro- and nanopowders with unique properties [15, 16]. To reduce the inductance of such circuits and obtain high dynamic parameters in them, the reverse pulse current can flow through the copper screen of the cables, that is, ordinary power cables can be used as coaxial.

In the electric power industry of Ukraine, modern power cables with LPE insulation and twisted and compacted aluminum multi-wire core are mostly used [7, 17]. To improve the plasticity and specific conductivity of such a wire, it must be «annealed», that is, subjected to a special heat treatment at temperature of about 420 °C for certain time, and then slowly cooled to bring the structure of aluminum products closer to an equilibrium state [18].

The practical and economic efficiency of using the «annealing» technology to improve the operational characteristics of aluminum conductive cores has already been confirmed by the authors of the article earlier when implementing the technology of passive heating of an aluminum core wound on a metal drum. Its passive heating was carried out from electric heaters located together with the core in a common thermal chamber. Currently, this technology of «annealing» of the aluminum core is used at YUZHCABLE WORKS, PJSC in the technological lines of serial production of modern low-voltage cables with aluminum core of increased plasticity and electrical conductivity.

However, in the technological lines of industrial production of modern domestic power cables for medium and high voltages, induction heating to 60–95 °C of the surface of the moving aluminum core of the cables with high-frequency current is already used to improve the quality of applying three-layer LPE insulation to it [7]. Therefore, it was important to evaluate the effectiveness of using induction units in such lines not only for relatively low-temperature heat treatment of the surface of aluminum cores, but also for increasing their plasticity and specific current conductivity.

In this work, a multi-turn inductor of small diameter (comparable to the diameter of the cable core) and relatively long (≥ 2 m) was investigated, in the harmonic magnetic field of which the cable core was moving. The electrical parameters of the inductor and the high-frequency power source were chosen in such a way that the core temperature at the output reached 420 °C.

Various modes of induction heat treatment of conductive materials and products were studied in numerous scientific publications [19-27]. In particular, in the publication of scientists of the world manufacturer of modern cable and wire heating systems Inductotherm Group Company [22], innovative inductor systems for simultaneous effective heating of single-conductor and multi-conductor cores of cables with justification for choosing the optimal frequency were investigated. The possibility of induction heating of conductors with diameter of 1.27 to 15.75 mm at power source frequency of 10 to 800 kHz is considered.

The article [23] shows ways to optimize induction heating using two types of inductors – flat and solenoid based on litz conductors. The optimal frequency for obtaining the maximum electrical efficiency was determined. It is shown that with fixed geometry and other system parameters, the efficiency of induction heating depends on the volume of copper in the windings. Experimental verification of the obtained results was carried out.

In [24], a transient electromagnetic-thermal model of induction heating of ferromagnetic materials was solved, taking into account their nonlinear dependencies (in particular, $B(H, T)$) and using the Finite Element Method. The multiphysics modeling strategy consisted in the fact that the electromagnetic problem was solved for fixed isothermal temperature fields, and the thermal problem was solved for the fixed heat of the heating source. The results of computer modeling of a ferromagnetic sample in a cylindrical inductor (with internal diameter of 50 mm and 5 turns) were confirmed by experimental studies of induction heating of material samples at three heating rates.

In the publication [25], the authors, using the Finite Element Method, conducted multiphysics modeling and experimental verification of the temperature distribution depending on the current frequency of the induction heater. A feature of the work is the manufacture of an inductor from a wire of the Litzendrat type and the use of relatively high frequencies from 15 to 25 kHz.

In [26], a study was conducted on the influence of the power of the induction heater, the feed rate, and the

diameter of the AISI 4140 steel sample on the temperature distribution in the samples depending on the diameter (7 mm, 14 mm, 21 mm, and 28 mm). An inductor in the form of a spiral coil with internal diameter of 5.8 cm was used, which heats the test sample in the temperature range from 492 °C to 746 °C. Two stages of heating are implemented – the first stage with ferromagnetic properties of the sample, and the second stage, when due to exceeding the Curie temperature, the sample becomes paramagnetic.

In the publication [27], the authors experimentally investigated the temperature distribution, heating rate, overheating, and temperature fluctuations of a commercial rod made of aluminum alloy 6061 with diameter of 10 mm and length of 1.5 m, with an analysis of the influence of heat treatment modes on the mechanical properties of the alloy. It is shown that the sample after induction heating to temperature of 560 °C has better mechanical properties compared to the sample heated in a conventional electric furnace.

One of the most important parameters of the efficiency of induction heating is the frequency of the power supply current of the inductor, at which its electrical efficiency reaches its maximum value. This frequency depends on many factors – the cross-sectional dimensions of the inductor turns, its overall dimensions and the air gap between the inductor and the core, as well as the material of the current-conducting core of the cables, its dimensions and other characteristic parameters. Considering the long length of such an inductor and, accordingly, the large number of turns (~ 100), the numerical calculation of the electromagnetic field and efficiency based on it, taking into account the geometric dimensions of the massive turns of the inductor in such a structure and the inhomogeneity of the electric current distribution in their volume, requires significant computer resources.

Features of simplifying computer calculations of the electromagnetic field and determining the efficiency in such systems were not considered in the above publications. In this article, to simplify calculations, the method of multiscale modeling [28–30] is used, which is based on the concept of an elementary cell containing only one inductor turn and a small core fragment located near this turn. At the same time, the action of the end effects in the inductor was not taken into account, because with its long length, they have a weak effect on the integral electromagnetic characteristics and the final value of the core temperature at the output of the inductor.

Thus, according to the multiscale modeling approach, the field problem was considered in the area of an elementary cell containing only one massive inductor turn and a core fragment. The equivalent R, L parameters of this cell were calculated as a function of the frequency of the power source, and then these results, by periodically repeating this cell, were transferred to the entire design of the inductor of the electro-induction heating installation.

The goal of the article is to develop, based on the method of multiscale modeling, a computer model for the analysis of electro-thermal processes in an induction plant for heating a moving aluminum core of a power cable to quantitatively assess the effectiveness of using such plants in existing industrial technological lines for the production of modern cables to increase the plasticity and specific conductivity of their aluminum cores.

One of the most important tasks was to obtain the frequency dependencies of the equivalent R, L parameters of such an inductor, taking into account the irregular distribution of electric current across its cross-section, and using them to determine the optimal frequency of the power source, which corresponds to the maximum value of the electrical efficiency of the inductor.

Research is aimed at assessing the possibility of achieving the goal in the industrial technological line of continuous application of modern three-layer cross-linked polyethylene insulation on the moving aluminum core of cables with voltage of up to 110 kV, which is serially manufactured by YUZHCABLE WORKS, PJSC.

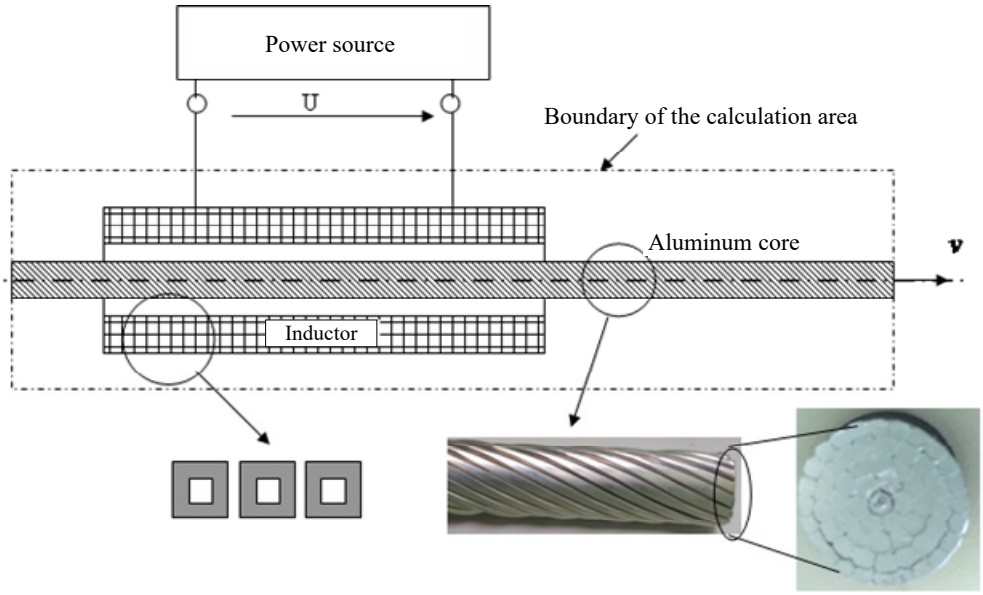

Fig. 1. Scheme of the physical model of the investigated installation for induction heating of the aluminum core of a power cable moving at constant speed v

Mathematical model of analysis of coupled electromagnetic and thermal processes. Figure 1 schematically shows the physical model of the investigated installation, which includes a relatively long water-cooled multi-turn inductor and an aluminum core of a power cable moving at constant speed v in the harmonic magnetic field of the inductor. When the inductor is connected to a power or high-frequency power source, induced electric currents arise in the core, and as a result of Joule heat release, it is heated.

A mathematical model for the analysis of coupled electromagnetic and thermal processes was constructed in the following approximation:

1. The consideration of the electromagnetic process was carried out in a steady state in the frequency domain, when all field characteristics are complex quantities. The thermal process was considered in the stationary mode.

2. In practice, the inductor is made of a copper tube and has a complex structure, which is conventionally shown in Fig. 1. However, at the first stage, when the main attention is paid to the thermal process in the core, the inductor can be considered as a multi-turn coil with given average electric current density $\dot{J}_i = \dot{I}_i N_i / S_i$, where $\dot{I}_i N_i$ is the MMF of the inductor, and S_i is its cross-sectional area. In this expression and below, complex quantities are indicated by a dot above.

3. The heated core is made of aluminum, is multi-wire and sealed. Its appearance and cross-section are shown in Fig. 1. The compaction coefficient reaches 0.96 and, as a result, it was considered solid in the calculations. Here, nonlinear dependencies of electrical conductivity, thermal conductivity, and specific heat capacity of its material on temperature were taken into account.

4. Taking into account the approximately cylindrical shape of the inductor and the core located symmetrically relative to the inductor, the problem was considered as axisymmetric, in a 2D formulation in the cylindrical coordinate system $r0z$ relative to the complex variable – the magnetic vector potential $\dot{A}(r, z)$, as well as the temperature $T(r, z)$ in the calculation area shown in Fig. 1.

This area contains three subareas – the inductor, the aluminum core, and the air surrounding these elements. The mathematical model that described the coupled electromagnetic and thermal processes included the formulation of electromagnetic and thermal problems, which are presented below.

The electromagnetic process was described by a system of differential equations for the complex value of the magnetic vector potential $\dot{A}$:

$$j\omega\sigma(T)\dot{A}_\varphi + \mu_0^{-1}\nabla\times(\nabla\times\dot{A}_\varphi) = 0 \text{, in the area of the core,} \quad (1)$$

$$\mu_0^{-1}\nabla\times(\nabla\times\dot{A}_\varphi) = \begin{cases} \dot{I}_i N_i / S_i, \text{ in the area of the inductor,} \\ 0, \text{ in air,} \end{cases} \quad (2)$$

where $\sigma(T)$ is the electrical conductivity of the core, which depends on the temperature, ω is the angular frequency of the current in the inductor, μ_0 is the magnetic constant.

As boundary conditions for the electromagnetic problem, the condition of symmetry with respect to the axis $r = 0$ and the condition of magnetic insulation on the outer boundary were set:

$$\dot{A}_\varphi|_C = 0. \quad (3)$$

The coupling between the electromagnetic problem and the thermal problem was carried out with the help of two quantities – he Joule heat release in the core q and the nonlinear dependence of the electrical conductivity of the core $\sigma(T)$.

The thermal problem for the unknown temperature distribution T included the following differential equation of heat transfer due to the mechanisms of heat conduction and convection:

$$\rho C_p(T)\boldsymbol{u}\cdot\nabla T - \nabla\cdot(\lambda(T)\nabla T) = \begin{cases} q, \text{ in the area} \\ \text{of the core,} \\ 0, \text{in other elements} \\ \text{of the area,} \end{cases} \quad (4)$$

where ρ, C_p, λ are the temperature-dependent density, specific heat capacity, and thermal conductivity of the material of the corresponding environment; $\boldsymbol{u} = (0, v)$ is the speed of movement of the core; q is the specific power of the heat source due to the induction heating of the core by the induced currents. It was defined as

$$q = \frac{\dot{J}\dot{J}^*}{\sigma} = \omega^2\sigma(\dot{A}_\varphi\cdot\dot{A}_\varphi^*), \quad (5)$$

where $\dot{J} = -j\omega\sigma\dot{A}_\varphi$ is the effective value of the induced current density; $\dot{A}_\varphi^*$ is the complex-conjugate magnitude of the magnetic vector potential.

The following were taken as boundary conditions for the thermal problem:

- on the axis of symmetry $r = 0$ – symmetry condition;
- on the outer boundary of the calculation area, as well as on the inlet (in the direction of movement) boundary of the core, the temperature is equal to the ambient temperature $T = T_0$;
- only convective heat transfer was set at the outlet boundary of the core;
- at the boundaries of the inductor, the temperature was assumed to be constant and equal to 70 °C, which is due to the presence of water cooling of the inductor turns.

The differential equations for the electromagnetic field (1), (2) and the temperature field (4) taking into account the specified boundary conditions represented a coupled electro-thermal problem that was solved numerically by the Finite Element Method using the Comsol software package [31]. The temperature dependencies of the values $\rho(T)$, $C_p(T)$, $\lambda(T)$ for the aluminum core was set according to the data of the material library of this code.

Analysis of the results of the calculation of the electro-thermal problem. The following parameter values were used in the calculations. The dimensions of the calculation area are 4.5 × 0.2 m. The length of the inductor is 2 m, the inner diameter is 40 mm, the number of turns $N_i = 50$. The current in the inductor was chosen on the condition that the core temperature at the exit from the inductor is approximately equal to the annealing temperature for aluminum T_{an} = 400–430 °C, the current frequency in the inductor varied from 50 to 5000 Hz. The diameter of the core is 28 mm, the speed of its movement is $v = 0.5$ m/min. Ambient air temperature $T_0 = 20$ °C.

Isolines of the magnetic vector potential $\dot{A}(r, z)$ and the distribution of magnetic flux density $|\dot{\boldsymbol{B}}|$ in the calculation area at current frequency of 50 Hz are shown in Fig. 2,*a*. The magnetic field is concentrated in the skin layer,

which at frequency of 50 Hz is $\delta = \sqrt{1/(\pi f \mu_0 \sigma)} = 15$ mm. Hence, Joule losses were allocated almost throughout the entire volume of the core, which led to its uniform heating throughout the thickness.

The temperature distribution in the calculation area is shown in Fig. 2,*b*, and in Fig. 2,*c* – temperature distribution along the *z* axis on the axis of symmetry (lower curve) and on the surface of the core (upper curve) at current frequency of 50 Hz.

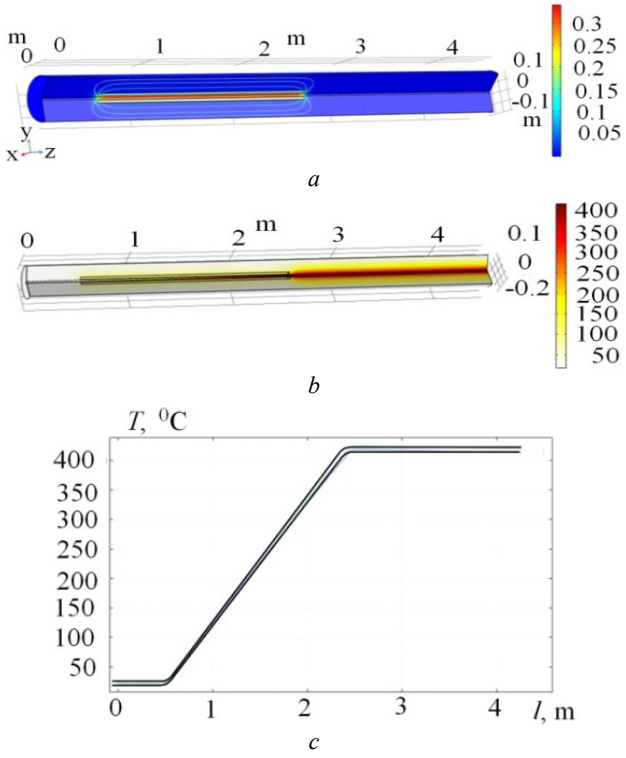

Fig. 2. Isolines of magnetic vector potential and distribution of magnetic flux density in the calculation area at current frequency of 50 Hz (*a*); temperature distribution in the calculation area (*b*); temperature distribution along the *z* axis on the axis of symmetry (lower curve) and on the surface of the core (upper curve) at current frequency of 50 Hz (*c*)

As can be seen from the results of the calculation, the temperature is regularly distributed along the depth of the core due to the small diameter of the core. Also, the temperature increases in the section «input – output from the inductor» according to a linear law, reaching the required annealing temperature 420 °C at the output.

The spatial distribution of the temperature at the output of the inductor is shown on a larger scale in Fig. 3. It should be noted that after leaving the inductor zone, the temperature distribution along the depth of the core does not become more uniform due to the cooling of the surface areas of the core.

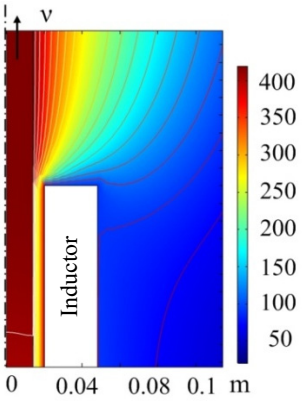

Fig. 3. Temperature distribution at the output from the inductor

To quantify the degree of irregular heating of the core along its depth, we can use the coefficient of temperature irregularity:

$$k_T = \frac{(T_{\max} - T_{\min})}{0{,}5(T_{\max} + T_{\min})} 100 \,, \qquad (6)$$

where $T_{\max}$, $T_{\min}$ are, respectively, the maximum and minimum temperature in the radial section of the core at the exit from the inductor. For the studied case according to Fig. 2,*c*, the value of $k_T = 1.6$ %.

Electromagnetic problem at the level of an elementary cell – at the micro level. The electro-thermal problem discussed above does not allow for a detailed analysis of electromagnetic processes in the inductor due to its relatively large length – the length/diameter ratio is 50. For such an analysis, an additional problem at the level of the elementary cell was further considered.

Figure 4 shows the structure of the inductor, which consists of massive copper coils made of a copper tube, which are cooled by a liquid pumped in this tube. Due to the long length of the inductor and the presence of a significant number of turns in its structure, an elementary cell was isolated, which included one turn of the inductor and a fragment of a core located near this turn (it is shown in Fig. 4 by a dotted line).

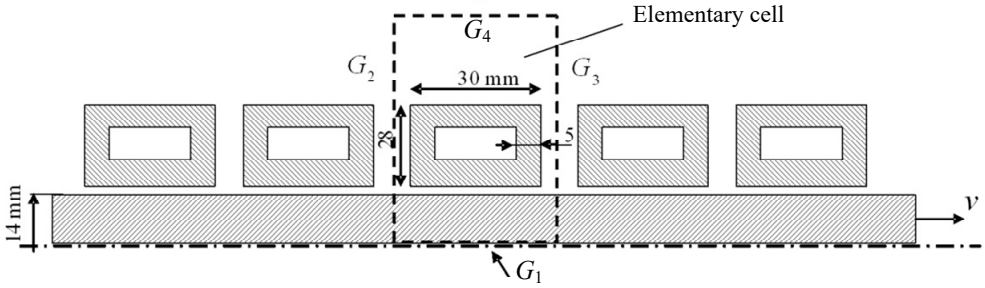

Fig. 4. Structure of a multi-turn inductor with a selected elementary cell

At the same time, it was assumed that the entire structure of the problem can be obtained by periodically repeating this cell along the *z* axis, and the total number of such cells is equal to the number of turns of the inductor N_i. Here, the action of the end effects in the inductor was not taken into account, however, with its long length,

these effects have a weak influence on the integral characteristics, and accordingly on the final value of the core temperature at the output of the inductor.

The dimensions of the inductor turns adopted in the calculations are shown in Fig. 4. It was assumed that all turns of the inductor are connected in series, and also that the core temperature in the cell region was equal to the average core temperature along its length of 220 °C.

Mathematical model of the electromagnetic problem in the area of the elementary cell in the approximation that the wire is stationary (the approximation of a small value of the magnetic Reynolds number) and assuming the validity of the axisymmetrical formulation has the following form:

- in the are of the core –

$$j\omega\sigma(T)\dot{A}_\varphi + \mu_0^{-1}\nabla\times(\nabla\times\dot{A}_\varphi) = 0\,; \tag{7}$$

- in the area of the inductor turn –

$$\begin{cases} j\omega\sigma\dot{A}_\varphi + \mu_0^{-1}\nabla\times(\nabla\times\dot{A}_\varphi) = \sigma\dfrac{\dot{U}_{turn}}{2\pi r}; \\ \displaystyle\int_{S_{\text{turn}}}\dot{J}dS = \dot{I}_{\text{turn}}, \quad \dot{J} = \sigma\left(\frac{\dot{U}_{turn}}{2\pi r} - j\omega\dot{A}_\varphi\right); \end{cases} \tag{8}$$

- in air –

$$\mu_0^{-1}\nabla\times(\nabla\times\dot{A}_\varphi) = 0\,, \tag{9}$$

where $\dot{U}_{turn}$ is the unknown voltage in the cross-section of the coil, which is calculated together with the magnetic vector potential $\dot{A}$ at given value of the electric current in the coil $\dot{I}_{turn}$. Since all turns of the inductor are connected in series, this current is equal to the current of the inductor $\dot{I}_i$, which is considered set.

The following boundary conditions were set for the electromagnetic problem (7)–(9): the symmetry condition with respect to the axis $r = 0$ at the boundary G_1 (see Fig. 4), the condition of even symmetry at the lateral boundaries G_2, G_3, and the condition of magnetic insulation at the outer boundary $G_4 - \dot{A}_\varphi|_{G_4} = 0$.

Figure 5 shows the distribution of the magnetic field $|\boldsymbol{B}|$, T (left) and the electric current density $|\boldsymbol{J}|$, A/m^2 (right) calculated in the Comsol code, in the cross-section of the elementary cell at different electric current frequency *f*. The current in the inductor coil was assumed to be 1 A.

The following effects can be seen from the presented figures:

- skin effect, when the magnetic field and electric current are displaced onto the surface of the conductor;
- proximity effect, when the presence of neighboring turns reduces the current on the side faces of the turn belonging to the cell;
- geometric effect, when due to the cylindrical structure of the coil, the electric current increases on its inner surface and decreases on its outer surface. Figure 5 shows how the manifestation of these effects increases with increasing frequency.

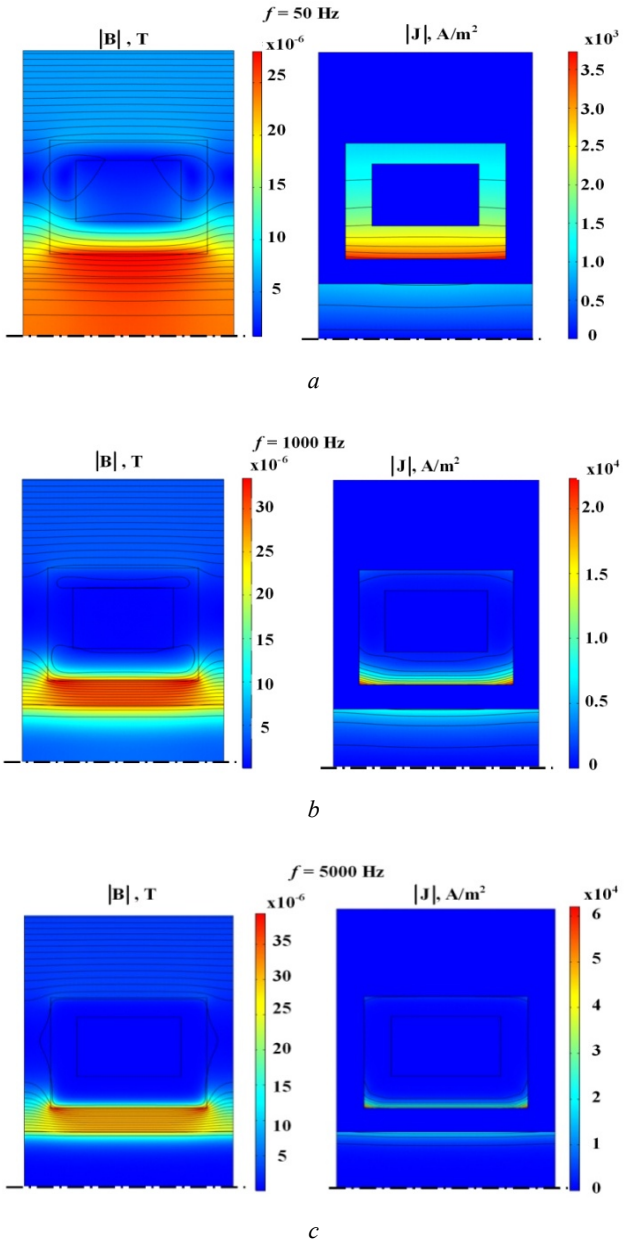

Fig. 5. Distributions of magnetic field (left) and density of electric current (right) in a cross-section of an elementary cells at the frequency of electric current: 50 Hz (*a*); 1000 Hz (*b*); 5000 Hz (*c*)

The distribution of the magnetic field in the inductor of a long length, which is studied in this problem, can be obtained by periodically repeating the pattern of the magnetic field for the cell – such patterns are shown in Fig. 6 for three values of the frequency of the power source. Note that this distribution will be valid for the internal areas of the inductor and will differ from the distribution in its end zones. But the use of such an approach, based on the calculation of the elementary cell field, allows to significantly simplify the problem of calculating the electromagnetic processes of long inductors, which is used in the task of induction heating of a power cable core.

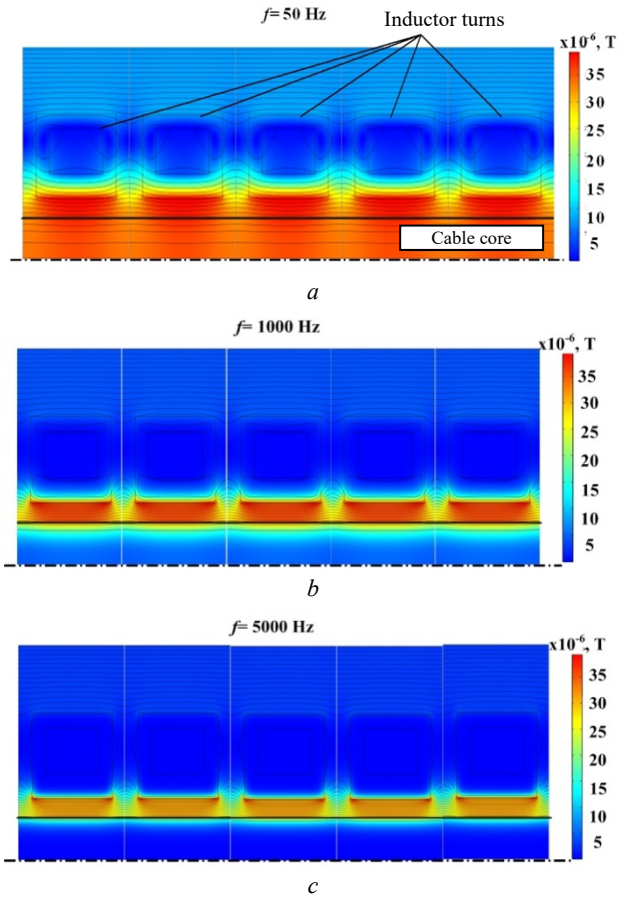

Fig. 6. Magnetic field distributions in inductor of large length at the frequency of electric current: 50 Hz (*a*); 1000 Hz (*b*); 5000 Hz (*c*)

Calculation of equivalent electrical parameters of one turn and multi-turn inductor as a whole. According to the results of the calculation of the electromagnetic field in the area of the elementary cell, the equivalent electrical parameters of one turn of the inductor as an element of this cell should be calculated depending on the frequency of the electric current. Here, the work uses a sequential replacing circuit of the turn (Fig. 7,*a*) and the multi-turn inductor as a whole (Fig. 7,*b*).

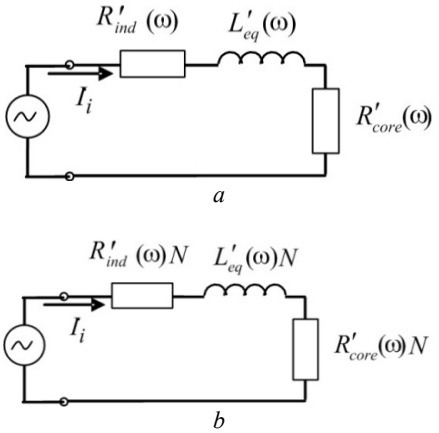

Fig. 7. Serial replacement circuits of: one turn (*a*); multi-turn inductor as a whole (*b*)

The replacing circuit of the multi-turn inductor with the number of turns N_i has the same structure as the circuit for the cell in Fig. 7,*a*, only the values of all parameters are multiplied by this number of turns N_i (Fig. 7,*b*).

These circuits contain the active resistance of the coil $R'_{ind}(\omega)$, the active resistance of the core fragment $R'_{core}(\omega)$ and the equivalent inductance $L'_{eq}(\omega)$, where $\omega = 2\pi f$ is the angular frequency of the electric current. Marking these elements with a dash means that they belong to one turn of the inductor.

The following expressions were used to calculate the frequency dependencies of these parameters:

$$R'_{ind}(\omega) = \frac{1}{I_i^2} \int\limits_{S_{turn}} \frac{\dot{J}\dot{J}^*}{\sigma} 2\pi r \mathrm{d}S\,, \tag{10}$$

$$R'_{core}(\omega) = \frac{1}{I_i^2} \int\limits_{S_{core}} \frac{\dot{J}\dot{J}^*}{\sigma} 2\pi r \mathrm{d}S\,, \tag{11}$$

$$L'_{eq}(\omega) = \frac{1}{I_i^2} \int\limits_{S_{cell}} \dot{B}\dot{H}^* 2\pi r \mathrm{d}S\,, \tag{12}$$

where S_{turn}, S_{core}, S_{cell} are, respectively, the surface of the turn, core and elementary cell.

Figure 8 shows the calculated frequency dependencies of these elementary cell parameters. The following can be concluded from them.

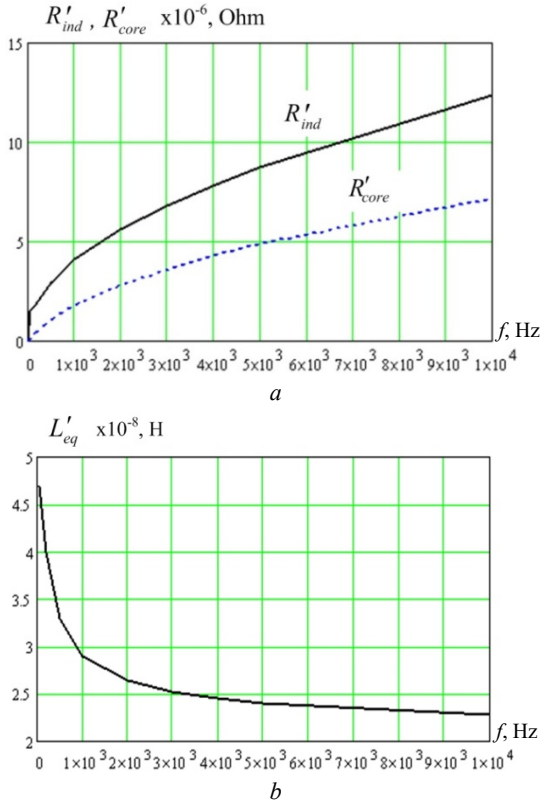

Fig. 8. Frequency dependencies of the parameters of the elementary cell: the active resistance of the turn $R'_{ind}(\omega)$ and the core fragment $R'_{core}(\omega)$ (*a*); the equivalent inductance $L'_{eq}(\omega)$ (*b*)

The equivalent resistance of the core at low frequency (< 50 Hz) approaches a small (zero) value, while the resistance of the winding $R'_{ind}(\omega)$ approaches the resistance at direct current.

Both resistances increase with increasing frequency and allow to calculate the electrical efficiency of the inductor as the ratio of losses in the core to the total losses – in the core and in the inductor.

The equivalent inductance of the cell decreases with the greatest speed in the frequency range of 50 Hz – 1000 Hz, when the magnetic field is intensively displaced into the air gap.

At higher frequencies, the inductance is caused mainly by the magnetic field in this gap and its decrease is significantly slowed down.

The use of the multi-turn inductor replacement circuit (Fig. 7,*b*) allows, using the electrical circuit for the high-frequency power source, to calculate the electrical processes in the installation for induction heating of the core at different power source frequencies.

Knowing the dependence of the equivalent active resistances of the turn and core on the frequency, it is possible to calculate the electrical efficiency of the inductor using the expression

$$\eta_i(\omega) = \frac{R'_{core}(\omega)}{R'_{core}(\omega) + R'_{ind}(\omega)}. \qquad (13)$$

The results of calculating the efficiency of the inductor as a function of the frequency of the power source obtained using the calculated active resistances shown in Fig. 8 are presented in Fig. 9 with a solid curve.

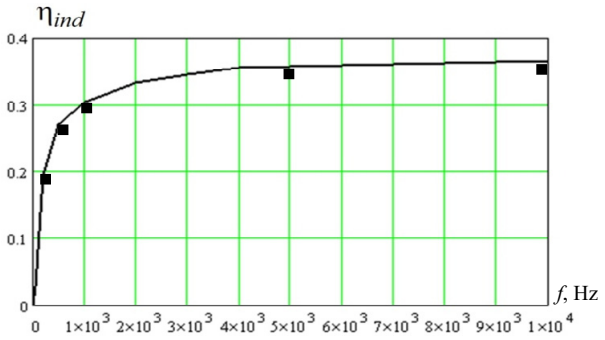

Fig. 9. Frequency dependence of the inductor efficiency as a result of the calculation for the elementary cell (solid curve) and for the inductor as a whole (marks ■)

It can be seen from this figure that the efficiency of heating the core at the power frequency is quite low, the electrical efficiency is equal to $\eta_{ind} = 0.028$. The optimal value of the frequency is 1–2 kHz and at the same time the electrical efficiency is $\eta_{ind} = 0.3$–0.33, respectively.

Although the electrical efficiency increases slightly with further frequency increase, losses in the semiconductor elements of the power source also increase, and therefore recommendations for increasing the frequency $f > 2000$ Hz require additional research.

The results of the calculation of the temperature field in the core at the optimal frequency of 1000 Hz show a uniform temperature distribution along the depth of the core at the exit from the inductor – the coefficient of temperature irregularity $k_T = 2$ %.

To verify the proposed computer model, built on the basis of the multi-scale modeling method, a 2D calculation of the electromagnetic problem was carried out for the entire calculation area, which includes a multi-turn inductor with massive turns, an aluminum core and an air region in a generally accepted way. The resulting distribution of the lines of force of the magnetic field in the calculation area for current frequency of 1000 Hz is shown in Fig. 10.

Fig. 10. Distribution of lines of force of the magnetic field in the cross-section of a multi-turn inductor at frequency of 1000 Hz

According to the results of the calculation, the total losses in the inductor and in the core were determined, and on their basis the electrical efficiency of the inductor $\eta_i(\omega)$ was calculated. The results of these calculations are shown in Fig. 9 with marks ■. A comparison of the results of calculations obtained using the elementary cell (solid curve) and when considering the inductor as a whole (shown by the mark ■) demonstrates the consistency of these results. At the same time, in order for calculation using the generally accepted method of the problem, the results of which are presented in Fig. 10, much more computer resources are required, and this is a feature of the calculation of relatively long inductors used in the technological processes of manufacturing current-conducting cores of power cables.

Table 1 shows the results of an experimental study of the characteristics of aluminum wire used at YUZHCABLE WORKS, PJSC in the manufacture of a conductive core, before and after the annealing process, realized by heating with electrodes in a special chamber with further exposure in a thermostat.

Table 1

Results of an experimental study of the characteristics of aluminum wire

Material – an aluminum core	Tear resistance, N/m^2	Relative elongation, %	Specific electrical resistance at 20 °C, Ω·m
Before annealing	177,9	2,0	$2{,}80 \cdot 10^{-4}$
After annealing	87,6	38	$2{,}77 \cdot 10^{-4}$

Increasing the plasticity of the aluminum core of power cables makes it possible to significantly speed up work on the restoration of PTLs of Ukraine in the war and post-war periods with the use of undamaged cable channels and trays and to increase the reliability of power supply systems of domestic critical infrastructure facilities.

Increasing the specific electrical conductivity of the aluminum core of cables additionally allows either to reduce its cross-section, and accordingly the volume of all active materials in the construction of power cables, or to additionally increase the reliability of power supply systems.

The results obtained in the article substantiate the expediency of creating an experimental model of the installation of high-frequency (1–2 kHz) induction heat treatment of the aluminum core of power cables at voltages up to 110 kV in order to clarify the technological and economic indicators of such heat treatment, in particular, when it is used in industrial lines of continuous application of modern three-layer cross-linked polyethylene insulation on the movable aluminum core of cables, which is serially manufactured by YUZHCABLE WORKS, PJSC, Kharkiv, Ukraine.

Conclusions.

Mathematical and computer models were developed for the analysis of electro-thermal processes in the installation of induction heating of the aluminum core of the power cable to implement the technological process of annealing this core. Taking into account the design features of the inductor for the implementation of such a process (in particular, the long length of the inductor and a significant number of its massive turns), the method of multi-scale modeling was used in the work.

Here, electro-thermal processes in the core were studied at the macro level, and at the micro level (that is, at the level of an elementary cell containing only one inductor turn and a core fragment) the distribution of the electromagnetic field and electric current density in the cross-section of the massive copper turn of the inductor was calculated, taking into account the features of its design. At both levels, the numerical Finite Element Method, implemented in the Comsol computer code, was used in the work.

According to the results of the calculation of the electromagnetic field at the level of the elementary cell, the frequency dependencies of the equivalent R, L parameters of the inductor were obtained, taking into account the skin effect, the proximity effect, and the geometric effect, and the quantitative influence of the electric current frequency on these effects was investigated.

The dependence of the electrical efficiency of the inductor on the frequency of the power source was obtained.

The analysis of the obtained numerical results showed that during the induction heat treatment of a movable aluminum core with diameter of 28 mm and the flow of currents in the inductor with frequency of up to 2 kHz, the efficiency of the heat treatment processes can exceed 30 % and temperature modes sufficient for annealing such a core without the use of a thermal insulation chamber can be realized.

To verify the proposed computer model, built on the basis of the multi-scale modeling method, a 2D calculation of the electromagnetic problem was carried out for the entire calculation area, which includes a multi-turn inductor with massive turns, an aluminum core and the surrounding air region in a generally accepted way. Comparison of the results of the calculations shows the consistency of the obtained results. At the same time, much more computer resources are needed to calculate the problem in a generally accepted way.

The obtained results substantiate the expediency of creating an experimental model of the installation of high-frequency (1–2 kHz) induction thermal annealing of the aluminum core of power cables to clarify the technological and economic indicators of its use in industrial lines of continuous application of modern three-layer cross-linked polyethylene insulation on the moving aluminum core of cables at voltage of up to 110 kV, which are mass-produced by YUZHCABLE WORKS, PJSC, Kharkiv, Ukraine.

Conflict of interest. The authors of the article declare that there is no conflict of interest.

REFERENCES

1. Kyrylenko O.V., Zhuikov V.Y., Denysiuk S.P. Use of dynamic tarification for optimization microgrid technical and economic indicators in local electricity markets. *Technical Electrodynamics*, 2022, no. 3, pp. 37-48. (Ukr). doi: https://doi.org/10.15407/techned2022.03.037.

2. Lezama F., Soares J., Hernandez-Leal P., Kaisers M., Pinto T., Vale Z. Local Energy Markets: Paving the Path Toward Fully Transactive Energy Systems. *IEEE Transactions on Power Systems*, 2019, vol. 34, no. 5, pp. 4081-4088. doi: https://doi.org/10.1109/TPWRS.2018.2833959.

3. Sinha A., Basu A.K., Lahiri R.N., Chowdhury S., Chowdhury S.P., Crossley P.A. Setting of Market Clearing Price (MCP) in Microgrid Power Scenario. *2008 IEEE Power and Energy Society General Meeting - Conversion and Delivery of Electrical Energy in the 21st Century*, 2008, pp. 1-8. doi: https://doi.org/10.1109/PES.2008.4596357.

4. Hirsch A., Parag Y., Guerrero J. Microgrids: A review of technologies, key drivers, and outstanding issues. *Renewable and Sustainable Energy Reviews*, 2018, vol. 90, pp. 402-411. doi: https://doi.org/10.1016/j.rser.2018.03.040.

5. Zolotarev V.M., Shcherba A.A., Karpushenko V.P., Peretiatko Yu.V., Zolotarev V.V., Oboznyi A.L. *Recommendations for the selection of characteristics, designs and application of self-carrying insulated wires produced by PJSC YUZHCABLE WORKS for overhead power lines of increased reliability and safety.* Kharkiv, Maidan Publ., 2008. 62 p. (Ukr).

6. Peschke E., Olshausen R. *Cable Systems for High and Extra-High Voltage*. MCD Verlag, 1999. 296 p.

7. Shydlovsky A.K., Shcherba A.A., Zolotariov V.M., Podoltsev A.D., Kucheriavaia I.N. *Polymer insulated cables for extra high voltage.* Kyiv, Institute of Electrodynamics National Academy of Sciences of Ukraine Publ., 2013. 550 p. (Rus).

8. Bezprozvannych G.V., Pushkar O.A. Increasing noise immunity of cables for fire protection systems. *Electrical Engineering & Electromechanics*, 2020, no. 4, pp. 54-58. doi: https://doi.org/10.20998/2074-272X.2020.4.07.

9. Kyrylenko O.V., Blinov I.V., Parus E.V., Trach I.V. Evaluation of efficiency of use of energy storage system in electric networks. *Technical Electrodynamics*, 2021, no. 4, pp. 44-54. (Ukr). doi: https://doi.org/10.15407/techned2021.04.044.

10. Nijman E., Buchegger B., Böhler E., Rejlek J. Experimental Characterization and Dynamic Modelling of Electrical Cables. *SAE International Journal of Advances and Current Practices in Mobility*, 2023, vol. 5, no. 2, pp. 888-896. doi: https://doi.org/10.4271/2022-01-0952.

11. Baranov M.I., Rudakov S.V. Electrothermal Action of the Pulse of the Current of a Short Artificial-Lightning Stroke on Test Specimens of Wires and Cables of Electric Power Objects. *Journal of Engineering Physics and Thermophysics*, 2018, vol. 91, no. 2, pp. 544-555. doi: https://doi.org/10.1007/s10891-018-1775-2.

12. Shazly J.H., Mostafa M.A., Ibrahim D.K., Abo El Zahab E.E. Thermal analysis of high-voltage cables with several types of insulation for different configurations in the presence of harmonics. *IET Generation, Transmission & Distribution*, 2017, vol. 11, no. 14, pp. 3439-3448. doi: https://doi.org/10.1049/iet-gtd.2016.0862.

13. Shcherba A.A., Suprunovska N.I. Electric energy loss at energy exchange between capacitors as function of their initial voltages and capacitances ratio. *Technical Electrodynamics*, 2016, no. 3, pp. 9-11. doi: https://doi.org/10.15407/techned2016.03.009.

14. Beletsky O.A., Suprunovska N.I., Shcherba A.A. Dependences of power characteristics of circuit at charge of supercapacitors. *Technical Electrodynamics*, 2016, no. 1, pp. 3-10. (Ukr). doi: https://doi.org/10.15407/techned2016.01.003.

15. Ochin P., Gilchuk A.V., Monastyrsky G.E., Koval Y., Shcherba A.A., Zaharchenko S.N. Martensitic Transformation in Spark Plasma Sintered Compacts of Ni-Mn-Ga Powders

Prepared by Spark Erosion Method in Cryogenic Liquids. *Materials Science Forum*, 2013, vol. 738-739, pp. 451-455. doi: https://doi.org/10.4028/www.scientific.net/MSF.738-739.451.
16. Vinnychenko D.V. Influence of electrical parameters of high-voltage electric-discharge systems for synthesis of nanocarbon on their performance and specific power inputs. *Technical Electrodynamics*, 2016, no. 4, pp. 95-97. (Ukr). doi: https://doi.org/10.15407/techned2016.04.095.
17. Ametani A., Xue H., Ohno T., Khalilhezhad H. *Electromagnetic Transients in Large HV Cable Networks: Modeling and calculations*. The Institute of Engineering Technology, 2021. 591 p. doi: https://doi.org/10.1049/PBPO204E.
18. Mokhort A.V., Chumak M.G. *Thermal processing of metals*. Kyiv, Lybid Publ., 2002. 512 p. (Ukr)
19. Rudnev V., Loveless D., Cook R. *Handbook of induction heating.* Boca Raton, CRS Press, 2017. 776 p. doi: https://doi.org/10.1201/9781315117485.
20. Sharma G.K., Pant P., Jain P.K., Kankar P.K., Tandon P. Numerical and experimental analysis of heat transfer in inductive conduction based wire metal deposition process. *Proceedings of the Institution of Mechanical Engineers, Part C: Journal of Mechanical Engineering Science*, 2022, vol. 236, no. 5, pp. 2395-2407. doi: https://doi.org/10.1177/09544062211028267.
21. Bao L., Wang B., You X., Li H., Gu Y., Liu W. Numerical and experimental research on localized induction heating process for hot stamping steel sheets. *International Journal of Heat and Mass Transfer*, 2020, vol. 151, art. no. 119422. doi: https://doi.org/10.1016/j.ijheatmasstransfer.2020.119422.
22. Mortimer J., Rudnev V., Clowes D., Shaw B. Intricacies of Induction Heating of Wires, Rods, Ropes & Cables. *Wire Forming Technology International*, Winter 2019, pp. 46-50.
23. Lope I., Acero J., Carretero C. Analysis and Optimization of the Efficiency of Induction Heating Applications With Litz-Wire Planar and Solenoidal Coils. *IEEE Transactions on Power Electronics*, 2016, vol. 31, no. 7, pp. 5089-5101. doi: https://doi.org/10.1109/TPEL.2015.2478075.
24. Fisk M., Ristinmaa M., Hultkrantz A., Lindgren L.-E. Coupled electromagnetic-thermal solution strategy for induction heating of ferromagnetic materials. *Applied Mathematical Modelling*, 2022, vol. 111, pp. 818-835. doi: https://doi.org/10.1016/j.apm.2022.07.009.
25. Siesing L., Frogner K., Cedell T., Andersson M. Investigation of Thermal Losses in a Soft Magnetic Composite Using Multiphysics Modelling and Coupled Material Properties in an Induction Heating Cell. *Journal of Electromagnetic Analysis and Applications*, 2016, vol. 08, no. 09, pp. 182-196. doi: https://doi.org/10.4236/jemaa.2016.89018.
26. Amarulloh A., Haikal H., Atmoko N.T., Utomo B.R., Setiadhi D., Marchant D., Zhu X., Riyadi T.W.B. Effect of power and diameter on temperature and frequency in induction heating process of AISI 4140 steel. *Mechanical Engineering for Society and Industry*, 2022, vol. 2, no. 1, pp. 26-34. doi: https://doi.org/10.31603/mesi.6782.
27. Shang F., Sekiya E., Nakayama Y. Application of High-Frequency Induction Heating Apparatus to Heat Treatment of 6061 Aluminum Alloy. *Materials Transactions*, 2011, vol. 52, no. 11, pp. 2052-2060. doi: https://doi.org/10.2320/matertrans.L-M2011825.
28. Podoltsev A.D., Kucheriavaia I.N. *Multiscale modeling in electrical engineering.* Kyiv, Institute of Electrodynamics National Academy of Sciences of Ukraine Publ., 2011. 255 p. (Rus).
29. Kovachki N., Liu B., Sun X., Zhou H., Bhattacharya K., Ortiz M., Stuart A. Multiscale modeling of materials: Computing, data science, uncertainty and goal-oriented optimization. *Mechanics of Materials*, 2022, vol. 165, art. no. 104156. doi: https://doi.org/10.1016/j.mechmat.2021.104156.
30. Ryu C.J., Kudeki E., Na D.-Y., Roth T.E., Chew W.C. Fourier Transform, Dirac Commutator, Energy Conservation, and Correspondence Principle for Electrical Engineers. *IEEE Journal on Multiscale and Multiphysics Computational Techniques*, 2022, vol. 7, pp. 69-83. doi: https://doi.org/10.1109/JMMCT.2022.3148215.
31. Available at: https://www.comsol.com (accessed 22 March 2023).

Received 11.04.2023
Accepted 29.06.2023
Published 02.01.2024

A.A. Shcherba[1], *Corresponding Member of the National Academy of Sciences of Ukraine, Doctor of Technical Science,*
O.D. Podoltsev[1], *Doctor of Technical Science*, *Chief Researcher,*
N.I. Suprunovska[1], *Doctor of Technical Science*, *Leading Researcher,*
R.V. Bilianin[2], *PhD*,
T.Yu. Antonets[2], *PhD*,
I.M. Masluchenko[3], *PhD*,
[1] Institute of Electrodynamics National Academy of Sciences of Ukraine,
56, Prospect Beresteiskyi, Kyiv-57, 03057, Ukraine,
e-mail: iednat1@gmail.com (Corresponding Author)
[2] YUZHCABLE WORKS, PJSC,
7, Avtogenna Str., Kharkiv, 61095, Ukraine.
[3] Scientific and Technical Center SE «NNEGC «Energoatom»,
22-24, Gogolivska Str., Kyiv, 01054, Ukraine.

How to cite this article:
Shcherba A.A., Podoltsev O.D., Suprunovska N.I., Bilianin R.V., Antonets T.Yu., Masluchenko I.M. Modeling and analysis of electro-thermal processes in installations for induction heat treatment of aluminum cores of power cables. *Electrical Engineering & Electromechanics*, 2024, no. 1, pp. 51-60. doi: https://doi.org/10.20998/2074-272X.2024.1.07